JPET Fast Forward. Published on September 19, 2017 as DOI: 10.1124/jpet.117.242503
This article has not been copyedited and formatted. The final version may differ from this version.

Discovery and Preclinical Characterization of GSK1278863 (daprodustat), A Small Molecule Hypoxia Inducible Factor (HIF)-Prolyl Hydroxylase Inhibitor for Anemia

Jennifer L. Ariazi, Kevin J. Duffy, David F. Adams, Duke Fitch, Lusong Luo, Melissa Pappalardi, Mangatt Biju, Erin Hugger DiFilippo, Tony Shaw, Ken Wiggall, Connie Erickson-Miller

GlaxoSmithKline, 709 Swedeland Road, King of Prussia, PA 19406 (JLA, DFA, DF, TS)

GlaxoSmithKline, 1250 South Collegeville Road, PA 19426 (KJD, MP, MB, KW)

while employed at GlaxoSmithKline, 1250 South Collegeville Road, PA 19426 (LL, EHDF, CE-M)

Running Title Page

Running title: **Preclinical Characterization of Daprodustat**

Corresponding Author:

Jennifer L Ariazi, GlaxoSmithKline, 709 Swedeland Road UW2230, King of Prussia, PA 19406

Tel: 610-270-5313

Fax: 610-270-5580

Email: jennifer.l.ariazi@gsk.com

Number of text pages: 26

Number of Tables: 3

Number of Figures: 8

Number of References: 74

Words in Abstract: 238

Words in Introduction: 719

Words in Discussion: 880

Non-standard Abbreviations: 2-OG, 2-oxoglutarate; α-KG, alpha-ketoglutarate; Alk5, activin receptor-like kinase 5; ARNT, aryl hydrocarbon receptor nuclear translocator, HIFβ; bhlh, basic helix loop helix; BSA, bovine serum albumin; CKD, chronic kidney disease; CODDD, C-terminal oxygen-dependent

degradation domain; CP4H, collagen prolyl hydroxylase; C-TAD, C-terminal transactivation domain; DFX, deferoxamine; DMEM, Dulbecco's Modified Eagle Medium; DMSO, dimethyl sulfoxide; DTT, dithiothreitol; EGLN, egg-laying nine; ELISA, enzyme-linked immunosorbent assay; EPO, erythropoietin; ESA, erythropoiesis stimulating agent; FBS, fetal bovine serum; FIH, factor inhibiting HIF; FIU, fluorescence intensity units; FLIPR, fluorimetric imaging plate reader; FRET, fluorescence resonance energy transfer; HBSS, Hanks balanced salt solution; HIF, hypoxia-inducible factor; HPLC, high performance liquid chromatography; HRE, hypoxia-response element; MSD, Meso-Scale Discovery; NODDD, N-terminal oxygen-dependent degradation domain; NOG, N-oxalylglycine; PAS, Per-Arnt-Sim; PHD, HIF prolyl hydroxylase; PPP, platelet-poor plasma; pVHL, von Hippel-Lindau tumor suppressor protein; rHuEPO, recombinant human erythropoietin; TBST, tris buffered saline containing 0.1% tween-20; ub, ubiquitin; VBC, von Hippel-Lindau protein-Elongin B-Elongin C; VEGF-A, vascular endothelial growth factor;

Recommended section assignment: Cardiovascular

ABSTRACT

Decreased erythropoietin (EPO) production, shortened erythrocyte survival, and other factors reducing the response to EPO contribute to anemia in patients with a variety of underlying pathologies such as chronic kidney disease (CKD). Treatment with recombinant human EPO (rHuEPO) at supraphysiological concentrations has proven to be efficacious. However, it does not ameliorate the condition in all patients and presents its own risks, including cardiovascular complications. The transcription factors hypoxia-inducible factor (HIF)1α and HIF2α control the physiological response to hypoxia and invoke a program of increased erythropoiesis. Levels of HIFα are modulated by oxygen tension via the action of a family of HIF-prolyl hydroxylases (PHDs) which tag HIFα for proteasomal degradation. Inhibition of these PHDs simulates conditions of mild hypoxia, leading to a potentially more physiological erythropoietic response, presenting a potential alternative to high doses of rHuEPO. Here we describe the discovery and characterization of GSK1278863, a pyrimidinetrione-glycinamide low nanomolar inhibitor of PHDs 1-3 which stabilizes HIFα in cell lines, resulting in the production of increased levels of EPO. In normal mice, a single dose of GSK1278863 induced significant increases in circulating plasma EPO but only minimal increases in plasma vascular endothelial growth factor (VEGF-A) concentrations. GSK1278863 significantly increased reticulocytes and red cell mass parameters in pre-clinical species following once-daily oral administration and has demonstrated an acceptable nonclinical toxicity profile supporting continued clinical development. GSK1278863 is currently in Phase 3 clinical trials for treatment of anemia in patients with CKD.

INTRODUCTION

Since its discovery as the hypoxia-induced complex responsible for erythropoietin (EPO) transcriptional regulation (Pugh et al., 1991; Semenza et al., 1991; Semenza and Wang, 1992), hypoxia-inducible factor (HIF) has been shown to recognize hypoxia-response elements (HREs) in many diverse genes (Schodel et al., 2011; Semenza, 2012). The HIF family includes three hypoxia-responsive proteins; HIF1α (Wang et al., 1995), HIF2α (Tian et al., 1997) and HIF3α (Makino et al., 2001). HIFα proteins form a heterodimer with HIFβ (Hoffman et al., 1991), resulting in a transcriptionally-active DNA binding complex. There is a large diversity of genes regulated by HIFα, (Schodel et al., 2011) with some cell-type and environment specificity in gene regulation (Ratcliffe, 2007; Loboda et al., 2010; Loboda et al., 2012; Mathieu et al., 2014). Dysregulation of HIF is associated with several pathologies, including cardiac failure (Wei et al., 2012; Bishop and Ratcliffe, 2015), stroke (Philipp et al., 2006; Bao et al., 2010), lung disease (Whyte and Walmsley, 2014), and retinal damage (Semenza et al., 2000; Arjamaa and Nikinmaa, 2006).

Under normoxia, HIFα is continually ubiquitinated and degraded by the proteasome (Figure 1). E3 ubiquitin ligase-mediated degradation of HIFα depends upon interaction with von Hippel-Lindau tumor suppressor protein (pVHL) (Maxwell et al., 1999) (Cockman et al., 2000). The oxygen-sensing mechanism controlling HIFα stabilization involves a family of HIF-prolyl hydroxylases (PHDs) (Epstein et al., 2001) which regulate the hydroxylation of conserved proline residues in HIFα, furnishing the essential recognition element for the HIFα -VHL interaction (Ivan et al., 2001; Jaakkola et al., 2001). The PHDs are members of the iron and α-ketoglutarate (α-KG)-dependent dioxygenase superfamily and are found in overlapping, but distinct tissue expression patterns (Lieb et al., 2002), with differences in subcellular localization. While the functional differences between the PHD isoforms are not well understood, mouse genetic knockout studies suggest they have distinct functions and phenotypes

(Minamishima et al., 2008; Takeda et al., 2008). In humans, a loss of function mutation in PHD2 was associated with familial erythrocytosis (Percy et al., 2006). PHD2 was found to be the primary regulator of HIF-1α levels in normoxia (Berra et al., 2003), while PHD3 was found to be the primary regulator of HIF2α, especially where PHD3 expression exceeded that of PHD2 under conditions of hypoxia (Appelhoff et al., 2004). Because the relative amounts of PHDs in EPO-producing cells *in vivo* are unknown, particularly in anemia, it is not clear which PHD or combination of PHDs should be inhibited to produce the best EPO-producing physiological response. To date, no isoform-selective, 2-KG-competitive PHD inhibitors have been reported.

HIF activity is further regulated by factor inhibiting HIF (FIH) (Mahon et al., 2001; Hewitson et al., 2002; Lando et al., 2002). FIH hydroxylates HIFα on an asparagine in the C-terminal transactivation domain (C-TAD), inhibiting HIFα's binding to its transcriptional coactivator, p300. FIH activity is prevalent under oxygen conditions lower than those where PHDs are active; investigation of the interplay of these systems in regulation of the hypoxic response is ongoing (Chan et al., 2016).

Inhibition of PHDs results in HIF stabilization and modulation of HIF-controlled gene products, including EPO. Therefore, approaches that target HIF stabilization through PHD inhibition and the production of physiological levels of endogenous EPO could alleviate anemia through increased reticulocyte production and subsequently increase erythrocyte levels, leading to increased hemoglobin and hematocrit levels and improved oxygen delivery (Forristal and Levesque, 2014). Furthermore, HIF affects iron metabolism modulators, including hepcidin (Yoon et al., 2006). A hepcidin decrease through PHD inhibition and hematopoiesis (Liu et al., 2012) may increase bioavailability of oral iron through increased absorption from the gut and allow better mobilization of iron stores from the liver and macrophages, potentially reducing or eliminating the need for iron supplementation often required for patients receiving rHuEPO.

Herein, we describe the discovery and preclinical development of GSK1278863, a potent PHD inhibitor which mimics the binding of N-oxalylglycine involving chelation of the catalytic iron and blocking substrate entry. We describe how enzymatic inhibition of PHD2 and PHD3 results in stabilization of cellular HIF1α and HIF2α, leading to production of EPO and subsequent induction of erythropoiesis *in vivo* in preclinical species. We also demonstrate selectivity of GSK1278863 against related enzymes, collagen prolyl hydroxylase (CP4H) and FIH, and describe an association established in nonclinical studies of structurally similar compounds between off-target activity on CP4H and development of cardiac valve lesions.

MATERIALS AND METHODS

GSK1278863 (2-(1,3-dicyclohexyl-6-hydroxy-2,4-dioxo-1,2,3,4-tetrahydropyrimidine-5-carboxamido) acetic acid) was synthesized as previously described (Duffy et al., 2007). All studies used the free acid form of the compound, GSK1278863A.

All studies were conducted in accordance with the GSK Policy on the Care, Welfare and Treatment of Laboratory Animals and were reviewed by the Institutional Animal Care and Use Committee either at GSK or by the ethical review process at the institution where the work was performed.

Western Blots for HIF Stabilization

The human hepatocellular carcinoma Hep3B cell line obtained from American Type Culture Collection (ATCC; Manassas, VA) was maintained in log phase growth by routine subcultivation in high glucose/glutamine Dulbecco's Modified Eagle Medium (DMEM) containing 10% fetal bovine serum (FBS) under standard culture conditions (37°C, 5% CO_2).

$2x10^6$ Hep3B cells were plated into P-100 cell culture dishes. After 48 hours, dishes were treated with 100 μM deferoxamine (DFX, positive control), or 25 or 50 μM GSK1278863 in fresh media. Dimethylsulfoxide (DMSO)-treated dishes (0.1%) were used as negative controls. Dishes were incubated for 6 hr in a CO_2 incubator at 37°C. Nuclear extract was prepared using the Nuclear Extract Kit according to the manufacturer's (Active Motif) instructions. Protein concentrations were determined using Bio-Rad protein assay reagent (Bradford method) with bovine serum albumin (BSA) at standard concentrations.

Protein samples were denatured at 99°C for 10 min in Laemmli sample buffer, resolved on a 7% Tris-Acetate gel and transferred to a nitrocellulose membrane. The blot was stained with Ponceau S to ensure equal loading. The membrane was washed and blocked with 10% Carnation milk in tris buffered saline containing 0.1% tween-20 (TBST) at room temperature for 20 min. The membrane was then incubated overnight at 4°C on a rocking platform with mouse monoclonal HIF-1α (Novus Biologicals NB100-105; 1:350) or rabbit polyclonal HIF-2α (Novus Biologicals NB100-122: 1:1000) antibodies diluted in 5% milk TBST. Blots were washed in TBST five times and incubated for 1 hr with donkey anti-rabbit IgG (GE Healthcare NA934; 1:2000) or sheep anti-mouse IgG (GE Healthcare NA931; 1:2000) conjugated to horseradish peroxidase. Antibody-protein complexes were then detected using ECL-Plus according to the manufacturer's (GE Healthcare) instructions.

Enzyme Assays

Materials

LANCE Eu-W8044 Streptavidin and α-[1-14C]-ketoglutaric acid were both purchased from PerkinElmer. HIF1α CAD peptide (D788-L822) was purchased from 21st Century Biochemicals. Dansyl-GFPG-Oet and (P-P-G)10 peptides were purchased from California Peptide Research. All other chemicals and materials were of standard laboratory grade. The following recombinant proteins were used for the biochemical assays: his-strep-tev-PHD2 (1-426), his-strep-tev-PHD1 (1-407), his-MBP-att-PHD3 (1-239), his-MBP-tev-FIH (1-349), Cy5-his-gb1-tev-HIF2α CODDD (467-572), Cy5-his-gb1-tev-HIF1α CODDD (498-603) and biotin-VBC complex (comprised of biotin-VHL, elongin b and elongin c). Detailed protein expression and purification information can be found in Pappalardi et al., 2008 and Pappalardi et al., 2011. Expression and purification of collagen prolyl hydroxylase (CP4H) was based on the methods described (Kersteen et al., 2004); however a baculovirus infected insect cell

(BIIC) expression system was utilized. The CP4H protein used for the biochemical assays was a tetramer comprised of full-length human collagen prolyl hydroxylase subunits A (P4HA) and B (P4HB).

LANCE Assay

Human PHD3 *in vitro* enzymatic activity was measured using a LANCE™ (Homogeneous Time-Resolved Fluorescence Quenching Assay based on lanthanide chelates) format. When hydroxylated, Cy5-HIF-2α C-terminal oxygen-dependent degradation domain (CODDD) was recognized by the biotin-labeled von Hippel-Lindau protein-Elongin B-Elongin C (VBC) complex. Addition of Europium (Eu)/streptavidin allowed detection of product formation by fluorescence resonance energy transfer, with a ratio of Cy5 to Eu fluorescence emission (LANCE ratio) as the ultimate readout. Assays were performed at room temperature in a 10 μL reaction in black 384-well Nunc non-binding assay plates pre-stamped with 100 nL compound in 100% DMSO. Reactions were performed by dispensing enzyme (5 μL PHD3; prepared as a 2X concentrate containing 4.0 nM PHD3, 0.2 mg/mL BSA, 400 μM ascorbic acid, 1.25 μg/mL $FeCl_2$, 0.3 mM CHAPS, and 50 mM KCl in 50 mM HEPES at pH 7.5 into the assay plates, incubating the plates for 30 minutes, and then adding substrate (5 μL HIF2α-CODDD; 2X concentrate contained 50 nM Cy5-labeled HIF2α-CODDD, 25 nM biotin-VBC, 1 μg/mL Strepavidin-Europium, 20 μM α-ketoglutarate, 0.3 mM CHAPS, and 50 mM KCl in 50 mM HEPES pH 7.5). Reactions were incubated for 30 minutes and then read on a Perkin Elmer Viewlux imager at an excitation wavelength of 360 nM and at emission wavelengths of 610 and 660 nM. The raw data values are the quotient of the signal intensities at 660 and 610 (LANCE Ratio), and inhibition in each assay well was calculated as a proportion of the high and low control wells. Final concentration of α-ketoglutarate in the assay was set to be equivalent to ~2x K_m^{app}.

The human PHD2 assay was performed similarly using the PHD2 protein isoform (the 2X enzyme solution contained 4.0 nM PHD2, 0.2 mg/mL BSA, 400 μM ascorbic acid, 1.25 μg/mL $FeCl_2$, 0.3 mM CHAPS, and 50 mM KCl in 50mM HEPES pH 7.5) and HIF1α protein (the 2X substrate solution contained 50 nM Cy5-labeled HIF1α-CODDD, 50 nM VBC, 1 μg/mL Strepavidin-Europium, 1 μM α-ketoglutarate, 0.3 mM CHAPS, and 50 mM KCl in 50 mM HEPES pH 7.5).

The human PHD1 assay was performed similarly using the PHD1 protein isoform (the 2X enzyme solution contained 10 nM PHD1, 0.2 mg/mL BSA, 400 μM ascorbic acid, 1.25 μg/mL $FeCl_2$, 0.3 mM CHAPS, 1 mM TCEP and 50 mM KCl in 50mM HEPES pH 7.5) and HIF1α protein (the 2X substrate solution contained 50 nM Cy5-labeled HIF1α-CODDD, 50 nM VBC, 1 μg/mL Strepavidin-Europium, 0.3 μM α-ketoglutarate, 0.3 mM CHAPS, and 50 mM KCl in 50 mM HEPES pH 7.5). Slight changes included the addition of 0.5 mM final TCEP to the reaction and plates were read on the Envision following a 40 minute reaction time.

A modified version of the screening assay was used to examine the mode of inhibition for GSK1278863. Using a 384-well plate (Corning #3637), PHD3/Cofactor mix (2.33X final concentration in 50 mM HEPES, pH 7.5 with 50 mM KCl) was incubated at room temperature for 1 minute with GSK1278863A (10 point, 3-fold serial dilution in 25% DMSO, 7X final concentration) or 25% DMSO. The enzymatic reaction was initiated upon the addition of substrate (2.33X final concentration) resulting in a final volume of 7 μL. LANCE ratio values were measured using a Perkin Elmer Envision (excitation at 320 nm, emission at 665 and 615 nm). Final concentrations of the PHD3/Cofactor mix consisted of 5 nM enzyme, 0.1 mg/mL BSA, 5 μM $FeCl_2$, 200 μM ascorbic acid, 70 nM biotin-VBC, 0.6 μg/mL Europium-Streptavidin, and 43 nM Cy5-HIF-2α CODDD. The top dose of GSK1278863A tested was 12.5 μM. The substrate mix consisted of a 5 point, 3-fold serial dilution in ddH_2O of α-ketoglutarate,

where the top concentration tested was 200 μM. Percent inhibition data was determined from the slope of the progress curve typically ranging from 5 – 40 min. The IC_{50} was determined by fitting the percent inhibition data to a two-parameter IC_{50} equation. GSK1278863 IC_{50} values were then plotted as a function of α- ketoglutarate concentration divided by its K_m^{app} to determine the inhibition pattern and calculate K_i^{app}. The data are best fit by the Cheng-Prusoff equation for competitive inhibition.

$$IC_{50} = K_i/(1+([S]/K_m) \quad \text{Eq. 1}$$

A second testing under similar conditions resulted in the same conclusion. PHD2 testing consisted of a 5 minute preincubation with GSK1278863A at a top dose of 80 μM. The final enzyme concentration of PHD2 was 2 nM, Cy5-HIF-1α CODDD (60 nM) was used in place of Cy5-HIF-2α CODDD, and the top α-ketoglutarate concentration tested was 6 μM.

Measurement of the intrinsic dissociation rate constant (k_{off}) of GSK1278863A from PHDs was determined by rapid dilution. Part 1a: PHD3/Cofactor mix (1.33X final concentration in 50 mM HEPES, pH 7.5 with 50 mM KCl) was incubated for 30 minutes with DMSO or 10X inhibitor (4X final concentration diluted in 50% DMSO) at room temperature in a deep-well 96 well plate. Following a 30 minute incubation, the reactions were diluted 100-fold with buffer plus cofactors (1.11X final concentration). The concentrations of PHD3 and 10X inhibitor were 0.6 and 2.5 μM respectively during the incubation and subsequently diluted to 6 and 25 nM. Part 1b: PHD3/Cofactor mix was diluted 100-fold (6 nM final) and then incubated with 10X inhibitor (2.5 μM) for 30 minutes. Part 2: 9 μL of the diluted incubation mixes from Part 1a and 1b were added to a 384-well plate (Corning #3637) containing 1 μL of substrate mix (10X final concentration in 50 mM HEPES, pH 7.5 with 50 mM KCl) with or without 0.1X inhibitor. LANCE ratio values were measured using a Perkin Elmer Envision (excitation at 320 nm, emission at 665 and 615 nm). Final concentrations after Part 2 of the reaction

consisted of 5.4 nM PHD3, 0.09 mg/mL BSA, 4.5 μM $FeCl_2$ and 180 μM ascorbic acid for the PHD3/Cofactor mix. GSK1278863A was tested at final concentrations of 2250 nM (10X) and 22.5 nM (0.1X). The substrate mix consisted of 35 nM biotin-VBC, 0.6 μg/mL Europium-Streptavidin, 35 nM Cy5-HIF-2a CODDD, and 60 μM α-ketoglutarate. Data reported as n=4 determinations, n=3 used the above conditions; whereas, n=1 was tested using 450 to 4.5 nM PHD3 and GSK1278863A where α-ketoglutarate was held at 500 mM. The half-life was determined by fitting the progress curve to a fixed steady state velocity equation for time-dependent inhibition.

$$[P]=vs*t + (vi-vs)/kobs*(1-exp(-kobs*t))+background \quad \text{Eq. 2}$$

PHD2 testing contained slight experimental adjustments to the PHD3 protocol. From Part 1a, a portion of the PHD2/DMSO sample was diluted with 100-fold dilution buffer containing either (1) 0X inhibitor, (2) 0.1X inhibitor or (3) 10X inhibitor while the PHD2/10X inhibitor sample was diluted with buffer containing 0X inhibitor only. Steps Part 1b and the addition of 0.1X inhibitor to the substrate mix in Part 2 were removed. Final concentrations after Part 2 were 1.08 nM PHD2, 900 nM α-ketoglutarate, and 35 nM Cy5-HIF-1α CODDD versus HIF-2α. GSK1278863A was tested at final concentrations of 112.5 nM (10X) and 1.13 nM (0.1X).

FIH

GSK1278863 (10 point, 3-fold serial dilution in 50% DMSO, 15X final concentration) or 50% DMSO was added to 1.1 mL MicroTubes in strips of 12 followed by the addition of human FIH/Cofactor mix (4X final concentration in 50 mM HEPES, pH 7.5 with 50 mM KCl). The enzyme plus inhibitor mix was incubated at room temperature for 30 minutes. Substrate mix (1.4X final concentration in 50 mM HEPES, pH 7.5 with 50 mM KCl) was added to the MicroTubes yielding a 32 μL final reaction volume.

JPET Fast Forward. Published on September 19, 2017 as DOI: 10.1124/jpet.117.242503
This article has not been copyedited and formatted. The final version may differ from this version.

Filter paper cut in strips of 12 and saturated with 30 mM $Ca(OH)_2$ were quickly added to the MicroTubes (without touching the reaction mix at the bottom of the tube) and capped. After 25 minutes, the filter paper was removed, placed in a vial with scintillation cocktail and the released $^{14}CO_2$ captured on the filter paper was counted in a liquid scintillation spectrometer. Final concentrations of the FIH/Cofactor mix were 50 nM enzyme, 0.25 mg/mL BSA, 10 μM $FeCl_2$, and 1 mM ascorbic acid. The substrate mix consisted of 200 μM HIF-1α (D788-L822), 10 μM α-keto[1-14C] glutarate and 50 μM α-ketoglutarate. The final concentration of α-ketoglutarate in the assay was set to be equivalent to ~2x K_m^{app}. Percent inhibition data were determined from the total counts after a 25 minute reaction. The IC_{50} value was determined by fitting the percent inhibition data to a two-parameter IC_{50} equation.

The ability of GSK1278863 to inhibit human FIH in a time-dependent manner was determined using the above experimental procedure in addition to an IC_{50} value determined following one minute enzyme plus inhibitor incubation.

Collagen Prolyl Hydroxylase

Human CP4H/Cofactor mix (4X final concentration in 50 mM HEPES, pH 7.5 with 50 mM KCl) was incubated at room temperature for 30 minutes with GSK1278863 (10 point, 3-fold serial dilution in 50% DMSO, 15X final concentration) or 50% DMSO. Substrate mix (1.4X final concentration in 50 mM HEPES, pH 7.5 with 50 mM KCl) was added to the plate yielding a 32 μL final reaction volume. After 20 minutes, the reaction was quenched by the addition of 0.67% final H_3PO_4. Product formation was detected using Reverse Phase High Performance Liquid Chromatography (HPLC; Ex 336nM and Em 517 nM). Final concentrations of the CP4H/Cofactor mix were 21.11 nM enzyme, 1 mg/mL BSA, 50 μM FeCl2, 2 mM ascorbic acid, 100 μM DTT, and 100 μg/mL catalase. The substrate mix consisted of 100 μM dansyl-GFPG-Oet, and 110 μM α-ketoglutarate. Percent inhibition data were determined from

JPET Fast Forward. Published on September 19, 2017 as DOI: 10.1124/jpet.117.242503
This article has not been copyedited and formatted. The final version may differ from this version.

the ratio of product to substrate after a 20 minute reaction. The IC_{50} value was determined by fitting the percent inhibition data to a two-parameter IC_{50} equation.

Inhibition by GSK1278863 against human CP4H was confirmed using the radioactive $^{14}CO_2$ release assay similar to that described for FIH; however, the reaction was stopped after 20 minutes. Final concentrations of the CP4H/Cofactor mix were 20 nM enzyme, 1 mg/mL BSA, 50 μM $FeCl_2$, 2 mM ascorbic acid, 100 μM dithiothreitol (DTT), and 100 μg/mL catalase. The substrate mix consisted of 100 μM (P-P-G)10, 20 μM α-keto[1-^{14}C] glutarate and 90 μM α-ketoglutarate. The final concentration of α-ketoglutarate in the assay was set to be equivalent to ~2x K_m^{app}.

Serotonin (5HT)-2 Receptors

Because 5-hydroxytryptamine 2B (5HT-2B) receptor agonism has been implicated in the pathogenesis of fenfluramine-induced valvulopathy in humans, we hypothesized it could be involved in the valve lesions we observed. SHSY5Y cells stably transfected with the appropriate 5HT2 receptor were plated in 384-well Nunc non-coated black walled, clear bottom plates with 16000 cells per well in 100 μL α minimum essential medium + ribonucleosides (Gibco Invitrogen) supplemented with 10% fetal bovine serum (Gibco Invitrogen) and 400 μg/mL Geneticin G418 (Gibco Invitrogen) and incubated overnight in a humidified incubator at 37°C and 5% CO_2. Cells were washed to remove all media. Fifty microliters of buffer (Hanks balanced salt solution [HBSS], 20 mM HEPES, 4.16 mM $NaHCO_3$, 2.5 mM probenecid, pH 7.4; Sigma) were added and then all but 10 μL was aspirated. Thirty microliters of loading dye (250 μM Brilliant Black, 2μM Fluo-4 diluted in HBSS buffer; Molecular Devices) were added, and the cells were returned to the incubator for an hour. An 11-point 1:4 dilution series of test compounds were then added to the cells using the fluorimetric imaging plate reader (FLIPR, Molecular Devices) and the plates were returned to the incubator to equilibrate for 30 minutes.

For agonist assays, 5HT was diluted in buffer at 0.1 mM and then diluted 4-fold in buffer to generate an 11-point serial dilution. Six microliters of the dilution series was transferred into 95 μL buffer. A signal test was performed on a yellow plate to check uniformity of the laser beam, with exposure length set to 0.05 seconds and varying light in the range of 0.5 to 0.8W to obtain an average signal of ~63000 fluorescence intensity units (FIU). A signal test was performed on the cell plate to check variability with exposure length set to 0.4 seconds and varying light in the range of 0.5 to 0.9 W to obtain a desirable signal of ~6000 to 10000 FIU. The following program was then run on the FLIPR: 0.4 second exposure length; read every second for 60 counts for the first sequence, first interval; read every 3 seconds for 20 counts for the second interval; 10 μL addition of fluid. EC_{50} values were determined from a four parameter logistic curve fit using ABase.

For antagonist assays, the following program was run on the FLIPR: 0.4 second exposure length; read every second for 60 counts for the first sequence, first interval; read every 3 seconds for 20 counts for the second interval; 10 μL addition of fluid. IC_{50} values were determined from a four parameter logistic curve fit using ABase.

Mouse Plasma EPO and Hematological Counts

B6D2F1/Crl mice were ordered from Charles River Laboratories.

EPO and VEGF

Normal female B6D2F-1 mice (n=6) were dosed by oral gavage with GSK1278863 at 60 mg/kg and blood was collected from euthanized animals by cardiac puncture into EDTA tubes. Vehicle-treated animals were sampled at 6 hours only. Platelet-poor plasma (PPP) was prepared for EPO & VEGF ELISA timecourse analysis as follows: Samples were centrifuged at 1000xg for 10 minutes and the

plasma fraction removed to a new tube. Plasma samples were further centrifuged at 10,000 x g for 10 min. The supernatant (PPP) was removed to a fresh tube and stored at -80°C. PPP samples were analyzed for EPO and VEGF protein concentrations using Meso-Scale Discovery (MSD) mouse enzyme-linked immunosorbent assay (ELISA) plates according to manufacturer's instructions and read on the MSD SECTOR Imager 6000.

Data from the MSD SECTOR Imager 6000 (n=1 well for each mouse) were imported into an Excel spreadsheet for analysis. Sample EPO and VEGF concentrations in pg/mL were determined from a regression fit of the EPO or VEGF standard curves. Averages and standard errors were calculated and plotted.

Blood Counts – Reticulocytes and Hemoglobin

Groups of five female B6D2F1 mice were dosed orally once per day with either vehicle (1% methylcellulose) or GSK1278863 at 3, 10 or 30 mg/kg. Animals were dosed for 8 consecutive days, and blood was collected from euthanized animals by cardiac puncture on day 9 into EDTA tubes. Samples were analyzed on the Advia blood analyzer to determine blood cell parameters.

Blood parameters were imported from the Advia 120 blood analyzer into an Excel spreadsheet for analysis using Hemacalc, an Excel macro. Means, standard deviations, and standard errors were calculated using standard formulas. P values were determined using Student's t-test on the square roots of the sample values. The standard errors from Hemacalc were used to display error bars on the graphs.

Screening 14 Day Oral Toxicity Studies

GSK1278863

Groups of male or female Sprague Dawley rats (4/group; obtained from Charles River Laboratories, Raleigh, NC) were given 0 (vehicle), or 10, 30, 60, 100, 250 or 500 mg/kg/day GSK1278863 in 1% methylcellulose once daily for up to 14 days by oral gavage.

Other PHD Inhibitors (Compounds A, B, C, D, E and F)

Four groups/compound of male Sprague Dawley rats (4/group) were given 0 (vehicle), or 3 dose levels/compound (ranging from 10 to 300 mg/kg/day) in 1% methylcellulose once daily for up to 14 days by oral gavage.

28 Day Oral Toxicity Studies (Compound A)

Five groups of male and female CD-1^{TM} mice (10/sex/group; obtained from Charles River Laboratories, Raleigh, NC) were given 0 (vehicle), or 4 dose levels (ranging from 3 to 100 mg/kg/day) in 1% methylcellulose once daily for up to 28 days by oral gavage.

Four groups of male and female beagle dogs (3/sex/group; obtained from Marshall BioResources, Inc., North Rose, NY) were given 0 (empty gelatin capsule), or 3 dose levels (ranging from 15 to 120 mg/kg/day) once daily for up to 28 days by oral capsule.

Toxicity studies included standard study endpoints: clinical observations, body weights, hematology and clinical chemistry, organ weights, macroscopic and microscopic observations, and toxicokinetics (performed on separate subsets of animals in the rodent studies).

RESULTS

Identification and Biochemical Characterization of GSK1278863

A novel series of pyrimidinetrione inhibitors was designed to potently inhibit the PHDs, forming tight-binding interactions with the catalytic iron and a co-factor-pocket arginine residue (Figure 2). GSK1278863 was ultimately identified after extensive optimization of potency, selectivity and DMPK properties (as described further below).

A high-throughput homogeneous fluorescence resonance energy transfer (FRET) assay was developed to measure human PHD enzymatic activity (Pappalardi et al., 2008; Pappalardi et al., 2011). The primary substrate is the HIF CODDD (Figure 3) which contains a proline residue hydroxylated by PHD. All biochemical studies conducted with PHD1 and PHD2 used HIF1α CODDD as the substrate while PHD3 utilized HIF2α CODDD. The HIF CODDD substrates are labeled with the fluorescent group Cy5. When hydroxylated, Cy5-HIF CODDD is recognized by the biotin-labeled VBC complex. Addition of a Europium (Eu)/streptavidin chelate results in proximity of Eu to Cy5 in the product, allowing for detection by FRET. A ratio of Cy5 to Eu fluorescence emission, the Lanthanide chelate excite (LANCE) ratio is the ultimate readout, as this normalized parameter has significantly less variance than the Cy5 emission alone.

The inhibitory mechanism of GSK1278863 against α-KG for PHD3 was examined by plotting GSK1278863 IC_{50} values as a function of α-KG concentration divided by its K_m^{app}. GSK1278863 IC_{50} values increased in a manner consistent with an α-KG-competitive mode of inhibition, where the data are best fit by the Cheng-Prusoff equation for competitive inhibition ($IC_{50} = K_i/(1+([S]/K_m))$ (Yung-Chi and Prusoff, 1973) yielding a K_i^{app} value of 92 nM for PHD3 (Figure 4, left panel). GSK1278863 demonstrated time-dependent inhibition against PHD3, evident by a large increase in potency following

JPET Fast Forward. Published on September 19, 2017 as DOI: 10.1124/jpet.117.242503
This article has not been copyedited and formatted. The final version may differ from this version.

a 30 minute enzyme:inhibitor preincubation, shifting the K_i^{app} from 92 nM (1 minute enzyme:inhibitor preincubation) to 1.8 nM (Table 1). The K_i^{*app} values of 1.8 and 7.3 nM calculated using the Cheng-Prusoff equation for competitive inhibition against PHD3 and PHD2 respectively may underestimate the true K_i (K_i^*) under these conditions if the EI* conformation was not fully obtained under the standard assay conditions which contained a 30 minute enzyme:inhibitor preincuation (Table 1).

To determine if the observed time-dependent behavior was the result of slow-binding reversible inhibition between GSK1278863 and PHD3, a preformed GSK1278863 – PHD3 complex was rapidly diluted into substrate mix where the α-KG concentration was roughly 6xK_m^{app} to prevent rebinding.(Copeland, 2005) Upon dilution, recovery of PHD3 activity was observed, indicating that GSK1278863 is a reversible inhibitor of PHD3. The observed rate of recovery, k_{obs}, was obtained by fitting the data to a single exponential model. Under experimental conditions, k_{obs} reflects the intrinsic dissociation rate (k_{off}) of the inhibitor from PHD3. The residence half-life value ($t_{½}$) is calculated from k_{off} based on the equation $t_{½} = 0.693/ k_{off}$; $t_{½}$ = 132 ± 19 min (n=4) for PHD3 (Figure 4, right panel). This $t_{½}$ value indicates that GSK1278863 does not dissociate instantaneously from the PHD3 enzyme, resulting in prolonged inhibition of PHD3 which may impact the *in vivo* pharmacologic activity of this compound. GSK1278863 was also found to be an α-KG competitive, reversible inhibitor of PHD2 with residence half-life, $t_{½}$ = 92 ± 43 min (n=2) (see Supplementary Data).

Since GSK1278863 was designed as a co-factor mimetic, its ability to inhibit additional members of the iron dependent, α-KG- dioxygenase superfamily was assessed. IC_{50} values were determined against human CP4H using a procollagen peptide substrate and human FIH using a HIF1α peptide (D_{788}-L_{822}) following a 30 minute enzyme plus inhibitor preincubation. The resulting IC_{50} values of 9.8 μM for FIH and > 200 μM for CP4H show that GSK1278863 is at least 1000-fold selective for PHDs (Table 1).

The Biology and Pharmacology of GSK1278863

Induction of EPO

The immediate downstream effect of PHD inhibition in a cellular context is HIFα subunit accumulation. Stabilization of HIF1α and HIF2α was determined by western blot of nuclear protein extracts after GSK1278863 treatment of Hep3B cells. Western blot analysis demonstrated that neither HIF1α nor HIF2α was detected in the vehicle-treated cells, and both HIF1α and HIF2α were visualized in the DFX positive control-treated cells. Treatment with either 25 or 50 μM GSK1278863 for six hours resulted in the accumulation of both HIF1α and HIF2α subunits (Figure 5). These results demonstrate that prolyl hydroxylase inhibition by GSK1278863 treatment of cells results in the immediate downstream effect, HIFα subunit stabilization.

Moving from an *in vitro* context to *in vivo*, normal female B6D2F1 mice were administered a single oral dose of GSK1278863 at 60 mg/kg, and blood samples were collected at intervals between 4 and 30 hours post-dose (n=6 mice/time point for GSK1278863-treated mice; vehicle-treated mice were sampled at 6 hours only). Following treatment with GSK1278863, EPO protein levels peaked at 12 hours post-dose (Figure 6), representing an 11.2-fold increase with a mean plasma concentration of 1303 pg/mL. Additionally, EPO values at all other time points remained elevated by 1.9- to 2.9-fold relative to vehicle-treated mice. VEGF concentrations remained generally unchanged across the timecourse and only slightly higher than those of vehicle-treated mice. These data indicate that a single 60 mg/kg dose of GSK1278863 results in a significant, but transient increase in circulating levels of EPO, with minimal impact on VEGF concentrations.

In Vivo Increases in Reticulocyte Count and Hemoglobin

The pharmacological consequence of repeated daily treatment of normal B6D2F1 mice with vehicle or GSK1278863 (3, 10, or 30 mg/kg/day) for 8 days is shown in Figure 7. Approximately 24 hours after the final dose, mice were euthanized and blood was collected by cardiac puncture and analyzed on the Advia Blood Analyzer. Statistically significant increases in reticulocytes were observed in compound-treated mice (211%, 544%, and 673% over placebo) administered 3, 10, and 30 mg/kg GSK1278863, respectively (Figure 7A).

Consistent with the observed reticulocyte increases, hemoglobin levels were also found to be significantly elevated (12%, 17%, and 13%) relative to vehicle-treated mice after dosing with 3, 10, and 30 mg/kg/day GSK1278863, respectively (Figure 7B). Red blood cell counts and hematocrit were statistically significantly elevated in mice as well. Similar responses in reticulocytes and red blood cell mass parameters were evident in rats, beagle dogs and cynomolgus monkeys following comparable treatment durations, with responses progressing as dosing duration became more chronic (data not shown).

Pharmacokinetics of GSK1278863 in different animal species

When dosed intravenously, GSK1278863 showed low blood clearance in the mouse, rat, dog and monkey [< 1% hepatic blood flow (Qh) in mouse and rat, ~ 3% Qh in dog and ~ 19% Qh in monkey] (Table 2). Steady state volume of distribution (~ 0.3-0.8 L/kg) was less than or approximately equal to total body water in all four preclinical species.

Pharmacokinetic parameters were also determined for GSK1278863 following oral suspension administration to rats (Table 3). Unless otherwise indicated, rats were fasted overnight prior to oral administration of GSK1278863. The systemic exposure of GSK1278863 was similar in the rat following oral solution dosing (1.6 mg/kg) and oral suspension dosing (31.1 mg/kg) of crystalline

GSK1278863, suggesting a minimal impact of solubility and dissolution rate on the bioavailability of the drug molecule. Similar favorable comparisons between orally dosing a solution versus a suspension of crystalline solid were observed in both mice and dogs (see Supplementary Tables 1 and 2).

Toxicology

In screening 14-day oral toxicity studies with once daily administration to Sprague-Dawley rats, GSK1278863 demonstrated an acceptable toxicity profile that supported candidate selection and continued development. In chronic oral toxicity studies, dose-limiting effects of GSK1278863 were the result of marked pharmacologically-mediated increases in hematocrit and consisted of generalized vascular congestion, thrombosis and/or multi-organ pathology. These findings are considered consequences of compromised blood flow and vascular perfusion consequent to high hematocrits and inferred high blood viscosity and represent a manageable clinical risk via the routine hematology monitoring and hemoglobin stopping criteria in place in clinical studies of GSK1278863.

In contrast, four compounds (Compounds A, B, C and D – Supplementary Figure 2) of similar chemical structure and comparable on-target potencies induced cardiac valve lesions in 14-day rat, or 28-day mouse and dog, oral toxicity studies. These lesions were observed in right and/or left atrioventricular valves and/or aortic valves and consisted of a spectrum of changes most notably including myxomatous thickening characterized by widened valve leaflets and/or neutrophilic or mixed inflammatory cell infiltrates [Figure 8]. These valve lesions were not associated with an attached thrombus, or thrombosis elsewhere in the heart, as has been described for the valvulopathy observed in 4-week rat toxicology studies conducted with the hyperglycosylated rHuEPO AMG-114 (Andrews et al., 2014a). Uncertainty over the relevance of these findings to humans resulted in an unfavorable risk assessment for continued

development of these four compounds. Since valvulopathies are commonly associated with several human connective tissue disorders (eg. Ehlers Danlos, Marfans) (Glesby and Pyeritz, 1989; Ha et al., 1994; Myllyharju and Kivirikko, 2001; Lincoln et al., 2006) which are characterized by mutations in collagens and/or collagen processing genes, it was hypothesized that inhibitory activity on the closely related enzyme, CP4H, may be contributory. Interestingly, these four compounds demonstrated moderate inhibitory activity on human CP4H (IC_{50}s of 2.5 to 63 μM; PHD:CP4H selectivity of 20 to 1000-fold).

Prioritizing PHD:CP4H selectivity in our compound selection criteria led to the discovery of GSK1278863 (human CP4H IC_{50} >200 μM; PHD:CP4H selectivity 12,500-fold), which did not cause valvulopathy in 14- or 28-day rat oral toxicity studies, or in dog or monkey studies of up to 9 months duration when dosed to maximum tolerated doses. In 3- and/or 6-month mouse and/or rat oral toxicity studies, a few GSK1278863-treated animals presented with thrombi in atria or ventricles that resulted in minimal secondary valve lesions in adjacent structures. Thromboses in these cases were considered complications from polycythemia. The resultant valvular changes were morphologically distinct in character and severity from those observed in studies with Compounds A thru D and were typical of those often observed in association with cardiac thrombosis.

In light of the implication of 5-hydroxytryptamine 2B (5HT-2B) receptor agonism in the pathogenesis of fenfluramine-induced valvulopathy in humans (Connolly et al., 1997), we tested GSK1278863 and Compounds A thru D for antagonism of 5HT-2A, -2B and -2C receptors, and for agonism of 5HT-2B and -2C receptors. Activities were mild (XC_{50}s > 10 μM) and comparable for all compounds, suggesting serotonergic receptor-mediated mechanisms as an unlikely factor.

JPET Fast Forward. Published on September 19, 2017 as DOI: 10.1124/jpet.117.242503
This article has not been copyedited and formatted. The final version may differ from this version.

Importantly, GSK1278863 and two subsequent candidates (Compounds E and F; human CP4H IC_{50}s > 200 μM) that did not cause valvulopathy in screening 14-day rat oral toxicity studies, increased hematocrits to magnitudes comparable to those induced by the four compounds that induced cardiac valve lesions (Compounds A thru D). This suggests that polycythemia and assumed increased blood viscosity were not significant or sole contributing factors in the valvulopathy observed in short-term studies, especially given the absence of valvular or cardiac thromboses. Thus, our experience suggests a plausible association between CP4H inhibitory activity and the cardiac valve lesions observed with several non-selective HIF-prolyl-hydroxylase inhibitors in 14- or 28-day dog and/or rodent oral toxicity studies.

JPET Fast Forward. Published on September 19, 2017 as DOI: 10.1124/jpet.117.242503
This article has not been copyedited and formatted. The final version may differ from this version.

DISCUSSION

Our search for novel and potent HIF prolyl hydroxylase inhibitors began using the validated principle of molecular mimicry. N-Oxalylglycine has long been used as an unreactive substrate mimetic to inhibit α-KG-utilizing enzymes such as the prolyl 4-hydroxylases (Figure 2) (Cunliffe et al., 1992; Mole et al., 2003; Hausinger, 2004). Extending this principle, several heteroaryl-glycinamides have been discovered as inhibitors of α-KG-utilizing dioxygenases using a heterocyclic ring nitrogen atom to form a five-membered chelate with the enzyme-bound iron (e.g. 4-hydroxy-8-iodoisoquinolin-3-yl)carbonyl]amino}acetic acid) (McDonough et al., 2006). We postulated that an inhibitor with the potential to form a six-membered chelate would form a strong interaction with the PHDs and result in potent inhibitors of this class of enzyme. As shown in Figure 2, GSK1278863 (a pyrimidinetrione-glycinamide) mimics the binding of N-oxalylglycine, however chelating the catalytic iron through the glycinamide carbonyl and an acidic ring hydroxyl group in a six-membered chelate. The specific ring substitutions on the pyrimidine nucleus of GSK1278863 were derived through an extensive lead-optimization campaign and provided an inhibitor with optimized biological profile and pharmaceutical properties for progression into clinical trials (Johnson et al., 2014; Brigandi et al., 2016; Holdstock et al., 2016; Akizawa et al., 2017); a full description of this campaign is outside the scope of the present discussion.

GSK1278863 is a novel small molecule agent, which stimulates erythropoiesis through inhibition of hypoxia-inducible factor (HIF)-prolyl hydroxylases (PHDs). GSK1278863 is a potent inhibitor of all three HIF prolyl hydroxylase isozymes, PHD1, PHD2 and PHD3, with K_i apparents in the single-digit nanomolar range. Inhibition of the HIF-regulatory prolyl hydroxylases causes the accumulation of HIFα transcription factors resulting in increased transcription of HIF-responsive genes. The downstream physiological consequences of this altered gene expression essentially simulate the body's natural

adaptive response to hypoxia. GSK1278863 is highly selective for the HIF-prolyl hydroxylases compared to related oxygen-dependent, α-KG-utilizing metalloenzymes, such as FIH and CP4H. GSK1278863 treatment of Hep3B cells induces downstream effects of HIF-prolyl hydroxylase inhibition, including stabilization of HIF1α and HIF2α, and induction of erythropoietin. A single oral dose of GSK1278863 leads to peak plasma EPO concentrations in mice within 12 hours while daily dosing of GSK1278863 in preclinical species (see supplemental data) leads to a robust pharmacodynamic response resulting in a significant increase in hemoglobin and associated erythroid parameters within 7-14 days.

In toxicity studies, GSK1278863 has demonstrated an acceptable safety profile and therapeutic window supporting clinical progression into Phase 3. Importantly, with several pre-candidate compounds, we observed an association between CP4H inhibitory potency and development of dog and/or rodent cardiac valve lesions. Although further work would be required to investigate this association, it seems plausible as CP4H plays a key role in collagen synthesis and triple-helix formation, which, if impaired, could impact the organization of extracellular matrix. For example, it has been reported that interference with fibroblast/interstitial cell-mediated matrix turnover can impact the integrity and repair of cardiac valves (Jaffe et al., 1981; Glesby and Pyeritz, 1989; Gamulescu et al., 2006; Hinton et al., 2006; Hakuno et al., 2009). This is exemplified by the observation that an activin receptor-like kinase 5 (Alk5) inhibitor, a potent anti-fibrosis agent, causes severe and irreversible cardiac valve lesions in rats (Anderton et al., 2011). Also, Andrews *et al*. have reported on erythropoiesis stimulating agent (ESA)-related valvulopathy in rats administered AMG-114 and several other recombinant human erythropoietins (Andrews et al., 2014a; Andrews et al., 2014b). The AMG-114-related rat valvulopathy was often accompanied by an attached thrombus. This was not the case for the four GSK PHD compounds that induced valvulopathy in short term studies. The Andrews *et al*. article suggests

JPET Fast Forward. Published on September 19, 2017 as DOI: 10.1124/jpet.117.242503
This article has not been copyedited and formatted. The final version may differ from this version.

increased hematocrit as a predisposing factor in ESA-related rat toxicities, including valvulopathy. Our experiences with several PHD inhibitors that caused valvulopathy in dogs and/or rodents point to a plausible association with off-target inhibitory activity on the closely related enzyme, CP4H. Importantly, GSK1278863A, the molecule in clinical trials, is 12,500-fold selective for PHDs over CP4H.

PHDs and CP4H belong to a growing enzyme superfamily of iron and α-ketoglutarate-dependent dioxygenases. The members of this enzyme superfamily play critical roles in hypoxic signaling, DNA repair, stress response mechanisms, lipid and growth factor metabolism and epigenetic modifications (Aravind and Koonin, 2001; Falnes et al., 2002; Chen et al., 2008; Yang et al., 2009; Aik et al., 2013; Johansson et al., 2014; Ichiyama et al., 2015). Among them, many are important targets for drug discovery and development. As most of the inhibitors of these enzymes are designed to mimic the binding of N-oxalylglycine involving chelation of the catalytic iron and competing for α-ketoglutarate binding (Joberty et al., 2016), our finding cautions that CP4H inhibition might be an undesirable off target activity.

In summary, we have described the preclinical development of the PHD inhibitor GSK1278863. It is a potent and selective inhibitor, demonstrating ~600 – 2,800-fold selectivity against FIH, and 12,500-fold selectivity against CP4H. GSK1278863 stabilized HIF1α and HIF2α in Hep3B cells, and led to production of EPO and subsequent increases in reticulocytes and hemoglobin *in vivo*. The therapeutic window provided by the demonstrated efficacy and acceptable safety margin supported the progression of GSK1278863 (daprodustat) into the clinic, where it has been evaluated in Phase I (NCT00750256, NCT01319006, NCT01376232, NCT01673555, NCT02348372) and Phase II (NCT01047397), and is in ongoing Phase III clinical trials (NCT02876835, NCT02879305) for the treatment of anemia of chronic kidney disease.

ACKNOWLEDGMENTS

All listed authors met the criteria for authorship set forth by the International Committee for Medical Journal Editors. The authors wish to acknowledge Erding Hu, Kendall Frazier and Tim Hart for their assistance with study management and critical review, and Tracy Gales for image support, all of whom are employees of GlaxoSmithKline.

AUTHORSHIP CONTRIBUTIONS

Participated in research design: Adams, Ariazi, Duffy, Erickson-Miller, Luo

Conducted experiments: Ariazi, Biju, Pappalardi

Contributed new reagents or analytic tools: Duffy, Fitch, Shaw, Wiggall

Performed data analysis: Adams, Ariazi, Duffy, Hugger, Luo, Pappalardi

Wrote or contributed to the writing of the manuscript: Adams, Ariazi, Duffy, Pappalardi

REFERENCES

Aik W, Demetriades M, Hamdan MK, Bagg EA, Yeoh KK, Lejeune C, Zhang Z, McDonough MA and Schofield CJ (2013) Structural basis for inhibition of the fat mass and obesity associated protein (FTO). *J Med Chem* **56**:3680-3688.

Akizawa T, Tsubakihara Y, Nangaku M, Endo Y, Nakajima H, Kohno T, Imai Y, Kawase N, Hara K, Lepore J and Cobitz A (2017) Effects of Daprodustat, a Novel Hypoxia-Inducible Factor Prolyl Hydroxylase Inhibitor on Anemia Management in Japanese Hemodialysis Subjects. *Am J Nephrol* **45**:127-135.

Anderton MJ, Mellor HR, Bell A, Sadler C, Pass M, Powell S, Steele SJ, Roberts RR and Heier A (2011) Induction of heart valve lesions by small-molecule ALK5 inhibitors. *Toxicol Pathol* **39**:916-924.

Andrews DA, Boren BM, Turk JR, Boyce RW, He YD, Hamadeh HK, Mytych DT, Barger TE, Salimi-Moosavi H, Sloey B, Elliott S, McElroy P, Sinclair AM, Shimamoto G, Pyrah IT and Lightfoot-Dunn RM (2014a) Dose-related differences in the pharmacodynamic and toxicologic response to a novel hyperglycosylated analog of recombinant human erythropoietin in Sprague-Dawley rats with similarly high hematocrit. *Toxicol Pathol* **42**:524-539.

Andrews DA, Pyrah IT, Boren BM, Tannehill-Gregg SH and Lightfoot-Dunn RM (2014b) High hematocrit resulting from administration of erythropoiesis-stimulating agents is not fully predictive of mortality or toxicities in preclinical species. *Toxicol Pathol* **42**:510-523.

Appelhoff RJ, Tian YM, Raval RR, Turley H, Harris AL, Pugh CW, Ratcliffe PJ and Gleadle JM (2004) Differential function of the prolyl hydroxylases PHD1, PHD2, and PHD3 in the regulation of hypoxia-inducible factor. *J Biol Chem* **279**:38458-38465.

Aravind L and Koonin EV (2001) The DNA-repair protein AlkB, EGL-9, and leprecan define new families of 2-oxoglutarate- and iron-dependent dioxygenases. *Genome Biol* **2**:RESEARCH0007.

Arjamaa O and Nikinmaa M (2006) Oxygen-dependent diseases in the retina: role of hypoxia-inducible factors. *Exp Eye Res* **83**:473-483.

Bao WK, Qin P, Needle S, Erickson-Miller CL, Duffy KJ, Ariazi JL, Zhao SF, Olzinski AR, Behm DJ, Teg P, Jucker BM, Hu ED, Lepore JJ and Willette RN (2010) Chronic Inhibition of Hypoxia-inducible Factor Prolyl 4-hydroxylase Improves Ventricular Performance, Remodeling, and Vascularity After Myocardial Infarction in the Rat. *J Cardiovasc Pharmacol* **56**:147-155.

Berra E, Benizri E, Ginouves A, Volmat V, Roux D and Pouyssegur J (2003) HIF prolyl-hydroxylase 2 is the key oxygen sensor setting low steady-state levels of HIF-1alpha in normoxia. *EMBO J* **22**:4082-4090.

Bishop T and Ratcliffe PJ (2015) HIF hydroxylase pathways in cardiovascular physiology and medicine. *Circ Res* **117**:65-79.

Brigandi RA, Johnson B, Oei C, Westerman M, Olbina G, de Zoysa J, Roger SD, Sahay M, Cross N, McMahon L, Guptha V, Smolyarchuk EA, Singh N, Russ SF, Kumar S and Investigators PHI (2016) A Novel Hypoxia-Inducible Factor-Prolyl Hydroxylase Inhibitor (GSK1278863) for Anemia in CKD: A 28-Day, Phase 2A Randomized Trial. *Am J Kidney Dis* **67**:861-871.

Chai D, Colon M, Duffy KJ, Fitch DM, Tedesco R and Zimmerman M (2007) PROLYL HYDROXYLASE ANTAGONISTS. *WO 2007/038571*.

Chan MC, Ilott NE, Schodel J, Sims D, Tumber A, Lippl K, Mole DR, Pugh CW, Ratcliffe PJ, Ponting CP and Schofield CJ (2016) Tuning the Transcriptional Response to Hypoxia by Inhibiting Hypoxia-inducible Factor (HIF) Prolyl and Asparaginyl Hydroxylases. *J Biol Chem* **291**:20661-20673.

Chen YH, Comeaux LM, Eyles SJ and Knapp MJ (2008) Auto-hydroxylation of FIH-1: an Fe(ii), alpha-ketoglutarate-dependent human hypoxia sensor. *Chem Commun (Camb)*:4768-4770.

Cockman ME, Masson N, Mole DR, Jaakkola P, Chang GW, Clifford SC, Maher ER, Pugh CW, Ratcliffe PJ and Maxwell PH (2000) Hypoxia inducible factor-alpha binding and ubiquitylation by the von Hippel-Lindau tumor suppressor protein. *J Biol Chem* **275**:25733-25741.

Connolly HM, Crary JL, McGoon MD, Hensrud DD, Edwards BS, Edwards WD and Schaff HV (1997) Valvular heart disease associated with fenfluramine-phentermine. *N Engl J Med* **337**:581-588.

Copeland RA (2005) Evaluation of enzyme inhibitors in drug discovery. A guide for medicinal chemists and pharmacologists. *Methods Biochem Anal* **46**:1-265.

Cunliffe CJ, Franklin TJ, Hales NJ and Hill GB (1992) Novel inhibitors of prolyl 4-hydroxylase. 3. Inhibition by the substrate analogue N-oxaloglycine and its derivatives. *J Med Chem* **35**:2652-2658.

Duffy KJ, Fitch DM, Jin J, Liu R, Shaw A, N, and Wiggall KJ (2007) PROLYL HYDROXYLASE INHIBITORS. *WO 2007/150011*.

Epstein AC, Gleadle JM, McNeill LA, Hewitson KS, O'Rourke J, Mole DR, Mukherji M, Metzen E, Wilson MI, Dhanda A, Tian YM, Masson N, Hamilton DL, Jaakkola P, Barstead R, Hodgkin J, Maxwell PH, Pugh CW, Schofield CJ and Ratcliffe PJ (2001) C. elegans EGL-9 and mammalian homologs define a family of dioxygenases that regulate HIF by prolyl hydroxylation. *Cell* **107**:43-54.

Falnes PO, Johansen RF and Seeberg E (2002) AlkB-mediated oxidative demethylation reverses DNA damage in Escherichia coli. *Nature* **419**:178-182.

Forristal CE and Levesque JP (2014) Targeting the hypoxia-sensing pathway in clinical hematology. *Stem Cells Transl Med* **3**:135-140.

Gamulescu MA, Chen Y, He S, Spee C, Jin M, Ryan SJ and Hinton DR (2006) Transforming growth factor beta2-induced myofibroblastic differentiation of human retinal pigment epithelial cells: regulation by extracellular matrix proteins and hepatocyte growth factor. *Exp Eye Res* **83**:212-222.

Glesby MJ and Pyeritz RE (1989) Association of mitral valve prolapse and systemic abnormalities of connective tissue. A phenotypic continuum. *JAMA* **262**:523-528.

Ha VT, Marshall MK, Elsas LJ, Pinnell SR and Yeowell HN (1994) A patient with Ehlers-Danlos syndrome type VI is a compound heterozygote for mutations in the lysyl hydroxylase gene. *J Clin Invest* **93**:1716-1721.

Hakuno D, Kimura N, Yoshioka M and Fukuda K (2009) Molecular mechanisms underlying the onset of degenerative aortic valve disease. *J Mol Med (Berl)* **87**:17-24.

Hausinger RP (2004) Fe(II)/+¦-Ketoglutarate-Dependent Hydroxylases and Related Enzymes. *Critical Reviews in Biochemistry and Molecular Biology* **39**:21-68.

Hewitson KS, McNeill LA, Riordan MV, Tian YM, Bullock AN, Welford RW, Elkins JM, Oldham NJ, Bhattacharya S, Gleadle JM, Ratcliffe PJ, Pugh CW and Schofield CJ (2002) Hypoxia-inducible factor (HIF) asparagine hydroxylase is identical to factor inhibiting HIF (FIH) and is related to the cupin structural family. *J Biol Chem* **277**:26351-26355.

Hinton RB, Jr., Lincoln J, Deutsch GH, Osinska H, Manning PB, Benson DW and Yutzey KE (2006) Extracellular matrix remodeling and organization in developing and diseased aortic valves. *Circ Res* **98**:1431-1438.

Hoffman EC, Reyes H, Chu FF, Sander F, Conley LH, Brooks BA and Hankinson O (1991) Cloning of a factor required for activity of the Ah (dioxin) receptor. *Science* **252**:954-958.

Holdstock L, Meadowcroft AM, Maier R, Johnson BM, Jones D, Rastogi A, Zeig S, Lepore JJ and Cobitz AR (2016) Four-Week Studies of Oral Hypoxia-Inducible Factor-Prolyl Hydroxylase Inhibitor GSK1278863 for Treatment of Anemia. *J Am Soc Nephrol* **27**:1234-1244.

Ichiyama K, Chen T, Wang X, Yan X, Kim BS, Tanaka S, Ndiaye-Lobry D, Deng Y, Zou Y, Zheng P, Tian Q, Aifantis I, Wei L and Dong C (2015) The methylcytosine dioxygenase Tet2 promotes DNA demethylation and activation of cytokine gene expression in T cells. *Immunity* **42**:613-626.

Ivan M, Kondo K, Yang H, Kim W, Valiando J, Ohh M, Salic A, Asara JM, Lane WS and Kaelin WG, Jr. (2001) HIFalpha targeted for VHL-mediated destruction by proline hydroxylation: implications for O2 sensing. *Science* **292**:464-468.

Jaakkola P, Mole DR, Tian YM, Wilson MI, Gielbert J, Gaskell SJ, Kriegsheim A, Hebestreit HF, Mukherji M, Schofield CJ, Maxwell PH, Pugh CW and Ratcliffe PJ (2001) Targeting of HIF-alpha to the von Hippel-Lindau ubiquitylation complex by O2-regulated prolyl hydroxylation. *Science* **292**:468-472.

Jaffe AS, Geltman EM, Rodey GE and Uitto J (1981) Mitral valve prolapse: a consistent manifestation of type IV Ehlers-Danlos syndrome. The pathogenetic role of the abnormal production of type III collagen. *Circulation* **64**:121-125.

Joberty G, Boesche M, Brown JA, Eberhard D, Garton NS, Humphreys PG, Mathieson T, Muelbaier M, Ramsden NG, Reader V, Rueger A, Sheppard RJ, Westaway SM, Bantscheff M, Lee K, Wilson DM, Prinjha RK and Drewes G (2016) Interrogating the Druggability of the 2-Oxoglutarate-Dependent Dioxygenase Target Class by Chemical Proteomics. *ACS Chem Biol* **11**:2002-2010.

Johansson C, Tumber A, Che K, Cain P, Nowak R, Gileadi C and Oppermann U (2014) The roles of Jumonji-type oxygenases in human disease. *Epigenomics* **6**:89-120.

Johnson BM, Stier BA and Caltabiano S (2014) Effect of food and gemfibrozil on the pharmacokinetics of the novel prolyl hydroxylase inhibitor GSK1278863. *Clin Pharmacol Drug Dev* **3**:109-117.

Kersteen EA, Higgin JJ and Raines RT (2004) Production of human prolyl 4-hydroxylase in Escherichia coli. *Protein Expr Purif* **38**:279-291.

Lando D, Peet DJ, Gorman JJ, Whelan DA, Whitelaw ML and Bruick RK (2002) FIH-1 is an asparaginyl hydroxylase enzyme that regulates the transcriptional activity of hypoxia-inducible factor. *Genes Dev* **16**:1466-1471.

Lieb ME, Menzies K, Moschella MC, Ni R and Taubman MB (2002) Mammalian EGLN genes have distinct patterns of mRNA expression and regulation. *Biochem Cell Biol* **80**:421-426.

Lincoln J, Lange AW and Yutzey KE (2006) Hearts and bones: shared regulatory mechanisms in heart valve, cartilage, tendon, and bone development. *Dev Biol* **294**:292-302.

Liu Q, Davidoff O, Niss K and Haase VH (2012) Hypoxia-inducible factor regulates hepcidin via erythropoietin-induced erythropoiesis. *J Clin Invest* **122**:4635-4644.

Loboda A, Jozkowicz A and Dulak J (2010) HIF-1 and HIF-2 transcription factors--similar but not identical. *Mol Cells* **29**:435-442.

Loboda A, Jozkowicz A and Dulak J (2012) HIF-1 versus HIF-2--is one more important than the other? *Vascul Pharmacol* **56**:245-251.

Mahon PC, Hirota K and Semenza GL (2001) FIH-1: a novel protein that interacts with HIF-1alpha and VHL to mediate repression of HIF-1 transcriptional activity. *Genes Dev* **15**:2675-2686.

Makino Y, Cao R, Svensson K, Bertilsson G, Asman M, Tanaka H, Cao Y, Berkenstam A and Poellinger L (2001) Inhibitory PAS domain protein is a negative regulator of hypoxia-inducible gene expression. *Nature* **414**:550-554.

Mathieu JR, Heinis M, Zumerle S, Delga S, Le Bon A and Peyssonnaux C (2014) Investigating the real role of HIF-1 and HIF-2 in iron recycling by macrophages. *Haematologica* **99**:e112-114.

Maxwell PH, Wiesener MS, Chang GW, Clifford SC, Vaux EC, Cockman ME, Wykoff CC, Pugh CW, Maher ER and Ratcliffe PJ (1999) The tumour suppressor protein VHL targets hypoxia-inducible factors for oxygen-dependent proteolysis. *Nature* **399**:271-275.

McDonough MA, Li V, Flashman E, Chowdhury R, Mohr C, Lienard BM, Zondlo J, Oldham NJ, Clifton IJ, Lewis J, McNeill LA, Kurzeja RJ, Hewitson KS, Yang E, Jordan S, Syed RS and Schofield CJ (2006) Cellular oxygen sensing: Crystal structure of hypoxia-inducible factor prolyl hydroxylase (PHD2). *Proc Natl Acad Sci U S A* **103**:9814-9819.

Minamishima YA, Moslehi J, Bardeesy N, Cullen D, Bronson RT and Kaelin WG, Jr. (2008) Somatic inactivation of the PHD2 prolyl hydroxylase causes polycythemia and congestive heart failure. *Blood* **111**:3236-3244.

Mole DR, Schlemminger I, McNeill LA, Hewitson KS, Pugh CW, Ratcliffe PJ and Schofield CJ (2003) 2-oxoglutarate analogue inhibitors of HIF prolyl hydroxylase. *Bioorg Med Chem Lett* **13**:2677-2680.

Myllyharju J and Kivirikko KI (2001) Collagens and collagen-related diseases. *Ann Med* **33**:7-21.

Pappalardi MB, Martin JD, Jiang Y, Burns MC, Zhao H, Ho T, Sweitzer S, Lor L, Schwartz B, Duffy K, Gontarek R, Tummino PJ, Copeland RA and Luo L (2008) Biochemical characterization of human prolyl hydroxylase domain protein 2 variants associated with erythrocytosis. *Biochemistry* **47**:11165-11167.

Pappalardi MB, McNulty DE, Martin JD, Fisher KE, Jiang Y, Burns MC, Zhao H, Ho T, Sweitzer S, Schwartz B, Annan RS, Copeland RA, Tummino PJ and Luo L (2011) Biochemical characterization of human HIF hydroxylases using HIF protein substrates that contain all three hydroxylation sites. *Biochem J* **436**:363-369.

Percy MJ, Zhao Q, Flores A, Harrison C, Lappin TR, Maxwell PH, McMullin MF and Lee FS (2006) A family with erythrocytosis establishes a role for prolyl hydroxylase domain protein 2 in oxygen homeostasis. *Proc Natl Acad Sci U S A* **103**:654-659.

Philipp S, Jurgensen JS, Fielitz J, Bernhardt WM, Weidemann A, Schiche A, Pilz B, Dietz R, Regitz-Zagrosek V, Eckardt KU and Willenbrock R (2006) Stabilization of hypoxia inducible factor rather than modulation of collagen metabolism improves cardiac function after acute myocardial infarction in rats. *Eur J Heart Fail* **8**:347-354.

Pugh CW, Tan CC, Jones RW and Ratcliffe PJ (1991) Functional analysis of an oxygen-regulated transcriptional enhancer lying 3' to the mouse erythropoietin gene. *Proc Natl Acad Sci U S A* **88**:10553-10557.

Ratcliffe PJ (2007) HIF-1 and HIF-2: working alone or together in hypoxia? *J Clin Invest* **117**:862-865.

Schodel J, Oikonomopoulos S, Ragoussis J, Pugh CW, Ratcliffe PJ and Mole DR (2011) High-resolution genome-wide mapping of HIF-binding sites by ChIP-seq. *Blood* **117**:e207-e217.

Semenza GL (2012) Hypoxia-inducible factors in physiology and medicine. *Cell* **148**:399-408.

Semenza GL, Agani F, Feldser D, Iyer N, Kotch L, Laughner E and Yu A (2000) Hypoxia, HIF-1, and the pathophysiology of common human diseases. *Adv Exp Med Biol* **475**:123-130.

Semenza GL, Nejfelt MK, Chi SM and Antonarakis SE (1991) Hypoxia-inducible nuclear factors bind to an enhancer element located 3' to the human erythropoietin gene. *Proc Natl Acad Sci U S A* **88**:5680-5684.

Semenza GL and Wang GL (1992) A nuclear factor induced by hypoxia via de novo protein synthesis binds to the human erythropoietin gene enhancer at a site required for transcriptional activation. *Mol Cell Biol* **12**:5447-5454.

Shaw AN, Duffy KJ, Miller WH, Myers AK and Zimmerman M (2008) N-SUBSTITUTED GLYCINE DERIVATIVES: PROLYL HYDROXYLASE INHIBITORS. *WO2008/089052*.

Takeda K, Aguila HL, Parikh NS, Li X, Lamothe K, Duan LJ, Takeda H, Lee FS and Fong GH (2008) Regulation of adult erythropoiesis by prolyl hydroxylase domain proteins. *Blood* **111**:3229-3235.

Tian H, McKnight SL and Russell DW (1997) Endothelial PAS domain protein 1 (EPAS1), a transcription factor selectively expressed in endothelial cells. *Genes Dev* **11**:72-82.

Wang GL, Jiang BH, Rue EA and Semenza GL (1995) Hypoxia-inducible factor 1 is a basic-helix-loop-helix-PAS heterodimer regulated by cellular O2 tension. *Proc Natl Acad Sci U S A* **92**:5510-5514.

Wei H, Bedja D, Koitabashi N, Xing D, Chen J, Fox-Talbot K, Rouf R, Chen S, Steenbergen C, Harmon JW, Dietz HC, Gabrielson KL, Kass DA and Semenza GL (2012) Endothelial expression of hypoxia-inducible factor 1 protects the murine heart and aorta from pressure overload by suppression of TGF-beta signaling. *Proc Natl Acad Sci U S A* **109**:E841-E850.

Whyte MK and Walmsley SR (2014) The regulation of pulmonary inflammation by the hypoxia-inducible factor-hydroxylase oxygen-sensing pathway. *Ann Am Thorac Soc* **11 Suppl 5**:S271-276.

Yang J, Ledaki I, Turley H, Gatter KC, Montero JC, Li JL and Harris AL (2009) Role of hypoxia-inducible factors in epigenetic regulation via histone demethylases. *Ann N Y Acad Sci* **1177**:185-197.

Yoon D, Pastore YD, Divoky V, Liu E, Mlodnicka AE, Rainey K, Ponka P, Semenza GL, Schumacher A and Prchal JT (2006) Hypoxia-inducible factor-1 deficiency results in dysregulated erythropoiesis signaling and iron homeostasis in mouse development. *J Biol Chem* **281**:25703-25711.

Yung-Chi C and Prusoff WH (1973) Relationship between the inhibition constant (KI) and the concentration of inhibitor which causes 50 per cent inhibition (I50) of an enzymatic reaction. *Biochemical Pharmacology* **22**:3099-3108.

FOOTNOTES

This work was supported by GlaxoSmithKline.

Reprint requests should be sent to Jennifer L. Ariazi at 709 Swedeland Road, King of Prussia, PA 19406, jennifer.l.ariazi@gsk.com.

FIGURE LEGENDS

Figure 1: Schematic diagrams of the oxygen-dependent, transcriptional regulation by HIFα. Under normoxia, prolyl hydroxylases utilize oxygen to hydroxylate proline residues on HIFα, enabling its VHL-mediated degradation via proteasomes (ub refers to ubiquitin). FIH hydroxylates an asparagine residue on HIFα, preventing it from binding its transcriptional coactivator, p300. However, under increasing levels of hypoxia, first prolyl hydroxylase activity, then FIH activity is diminished, resulting in accumulation of HIFα and interaction with p300, leading to transcription of HIF-responsive genes, including those responsible for upregulation of erythropoiesis.

Figure 2: GSK1278863 and isoquinolineglycinamide binding compared to 2-oxoglutarate (2-OG) and N-oxalylglycine (NOG). 2-OG and NOG along with isoquinolineglycinamides form 5-membered chelates with the catalytic iron residue. GSK1278863 is designed to form a 6-membered chelate with iron. All molecules form a conserved salt bridge with the co-factor binding pocket arginine residue.

Figure 3: Schematic diagrams of HIF1α and HIF2α protein structure motifs. CODDD: C-terminal oxygen-dependent degradation domain; NODDD: N-terminal oxygen-dependent degradation domain; CAD: C-terminal activation domain; bHLH: basic helix-loop-helix; PAS: Per-Arnt-Sim domain

Figure 4: Mode of inhibition against PHD3 (left) where GSK1278863 IC_{50} values were plotted as a function of [α-KG]/K_m^{app} and fit to an equation for competitive inhibition. Determination of the dissociation half-life value ($t_{1/2}$) for GSK1278863 from PHD3 by rapid dilution method (right). The yellow squares show the enzyme activity after dilution fit to an equation to determine the observed rate of recovery (k_{obs}). Control reactions at 10x IC_{50} (filled diamonds) and 0.1x IC_{50} (open squares) represent enzyme activity prior to dilution and after dilution if the compound was rapidly reversible

Figure 5: HIF1α and HIF2α Stabilization in Hep3B Cells after Treatment with GSK1278863. Nuclear extracts were prepared from Hep3B cells treated for 6 hours as indicated and Western blots were performed to detect HIF1α and HIF2α. Equal amount of nuclear lysate were loaded to each lane for the western blot. Under normoxic conditions, HIF1α and HIF2α were not present, but both were detected after treatment with GSK1278863 or DFX, with a possible concentration-dependent increase of HIF1α.

Figure 6: EPO and VEGF in Plasma of Mice Treated with Vehicle or a Single Oral 60 mg/kg Dose of GSK1278863. Normal female B6D2F1 mice (n=6) were administered a single oral dose of 60 mg/kg of GSK1278863, and platelet-poor plasma was collected at the indicated timepoints. Platelet-poor plasma was collected 6 hours after vehicle treatment. EPO and VEGF were detected by MSD ELISA. Averages and standard errors are depicted.

Figure 7: Mouse Reticulocytes and Hemoglobin after 8 daily oral doses of GSK1278863. Normal female B6D2F1 mice (n=5) were administered 8 daily oral doses of vehicle or GSK1278863at the doses indicated. Blood was analyzed on an Advia blood analyzer, and the means and standard errors are plotted.

Figure 8: Representative photomicrographs of Movat's pentachrome-stained heart sections from 28 day mouse oral toxicity study with Compound A showing myxomatous thickening (asterisks) of the aortic valve primarily due to increased proteoglycan matrix (blue staining); A). control mouse, B). treated mouse. a = aortic wall

JPET Fast Forward. Published on September 19, 2017 as DOI: 10.1124/jpet.117.242503
This article has not been copyedited and formatted. The final version may differ from this version.

TABLES

Table 1: Inhibitory activity of GSK1278863 against α-KG-dependent iron dioxygenases following a 30 minute enzyme:inhibitor preincubation. K_i^{app} values were calculated based on the equation: $K_i = IC_{50}/(1+([S]/K_m)$ for a competitive inhibitor.(Yung-Chi and Prusoff, 1973)

Enzyme	Substrate	α-KG K_m (nM)	IC_{50} ± StDev (nM)	$K_{i\ app}$ (nM)	n	Assay Format
PHD1	HIF1α CODDD	71 ± 12[a]	3.5 ± 0.6	1.8 ± 0.3	2	FRET
PHD2	HIF1α CODDD	188 ± 14 [a]	22.2 ± 13.4	7.3 ± 4.5	10	FRET
PHD3	HIF2α CODDD	7500 ± 2000 [a]	5.5 ± 5.1	1.8 ± 1.7	10	FRET
FIH	HIF-1α (D_{788}-L_{822})	32 ± 6	9,800 ± 7,500	3,200 ± 2,500	2	$^{14}CO_2$ Capture
CP4H	Procollagen peptide	53 ± 1	> 200,000	> 63,000	7	HPLC/$^{14}CO_2$

[a]Reported in Pappalardi et al. 2011.

JPET Fast Forward. Published on September 19, 2017 as DOI: 10.1124/jpet.117.242503
This article has not been copyedited and formatted. The final version may differ from this version.

Table 2: Summary of the pharmacokinetics of GSK1278863[a]

Species	CL[b] (mL/min/kg)	V_{dss} (L/kg)	$T_{1/2}$ (hours)	MRT (hours)	Oral F (%)
Mouse[b]	0.7	0.3	ND	7.8	88
Rat	0.2 ± 0.02	0.4 ± 0.1	33.5 ± 6.2	36.7 ± 4.7	~100[c]
Dog	0.9 ± 0.2	0.5 ± 0.1	6.6 ± 2.1	8.8 ± 2.7	46 ± 6
Monkey	8.4 ± 0.2	0.8 ± 0.1	1.9 ± 0.1	1.6 ± 0.1	34 ± 8

[a]Mean and standard deviation of parameter, where appropriate (n=3); [b]Composite sampling design (n=3 animals per time point). [c]Non-crossover design, data estimated from mean iv data. ND = not determined.

JPET Fast Forward. Published on September 19, 2017 as DOI: 10.1124/jpet.117.242503
This article has not been copyedited and formatted. The final version may differ from this version.

Table 3: Mean oral pharmacokinetic parameters of GSK1278863 in the rat[a]

Dose (mg/kg)	Cmax (μg/mL)	Tmax[b] (hours)	AUC0-24h (μg.h/mL)	AUC0-inf (μg.h/mL)	DNAUC0-24h[c] (μg.h/mL/mg/kg)
1.6[d]	2.86 ± 0.51	4.0	46.61 ± 8.95	106.63 ± 19.97	29.13
31.1[e,f]	62.40 ± 3.78	2.0	941.02 ± 68.91	ND	30.26

[a]Mean and standard deviation of parameter, where appropriate (n = 3); serial sampling design in male Sprague-Dawley rats. [b]Tmax expressed as median. [c]Dose-normalized AUC(0-24h). [d]Solution in 2% DMSO, 20% (w/v) Captisol® in water, pH~7.0. [e]Suspension in 1% methylcellulose. [f]Animals were not fasted overnight prior to dosing. ND: not determined since % extrapolated AUC(0-inf) was high.

JPET Fast Forward. Published on September 19, 2017 as DOI: 10.1124/jpet.117.242503
This article has not been copyedited and formatted. The final version may differ from this version.

Figure 1:

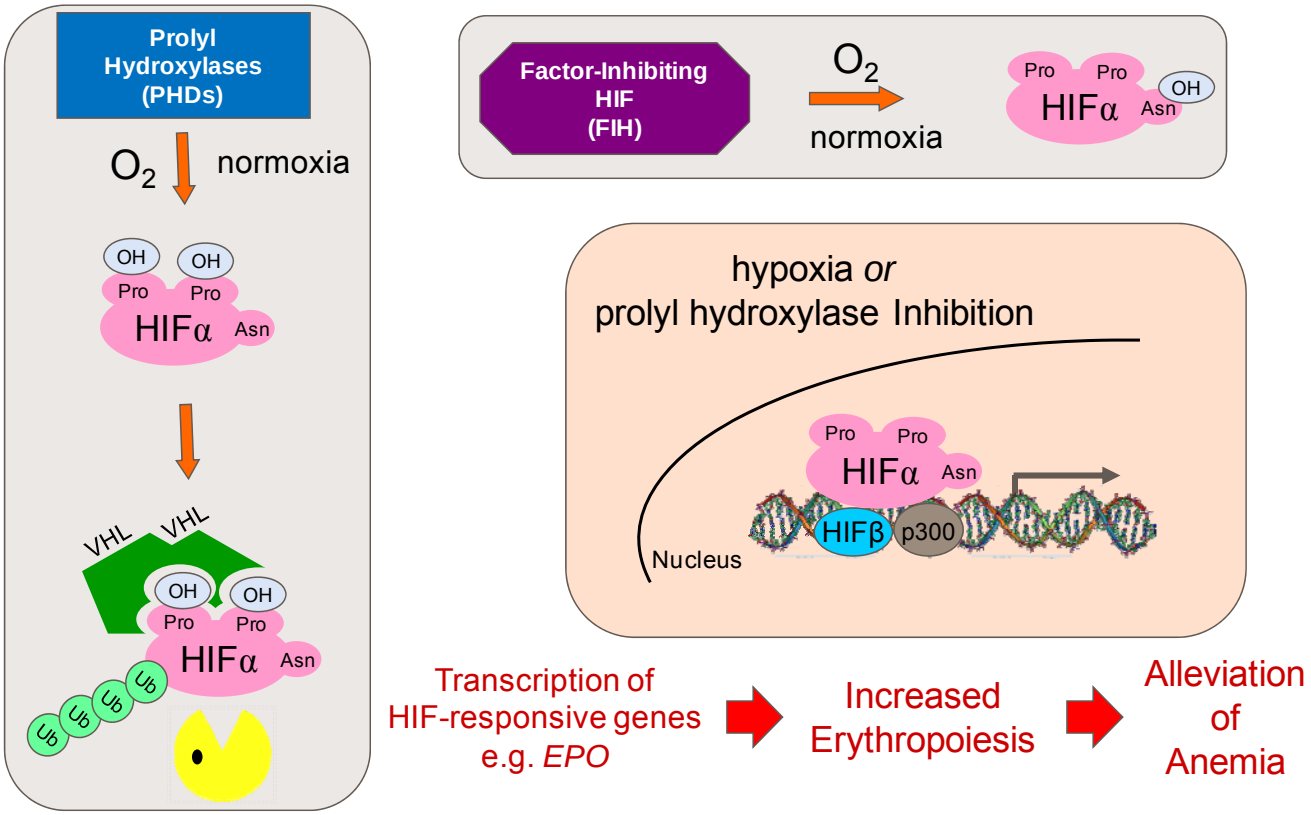

JPET Fast Forward. Published on September 19, 2017 as DOI: 10.1124/jpet.117.242503
This article has not been copyedited and formatted. The final version may differ from this version.

Figure 2

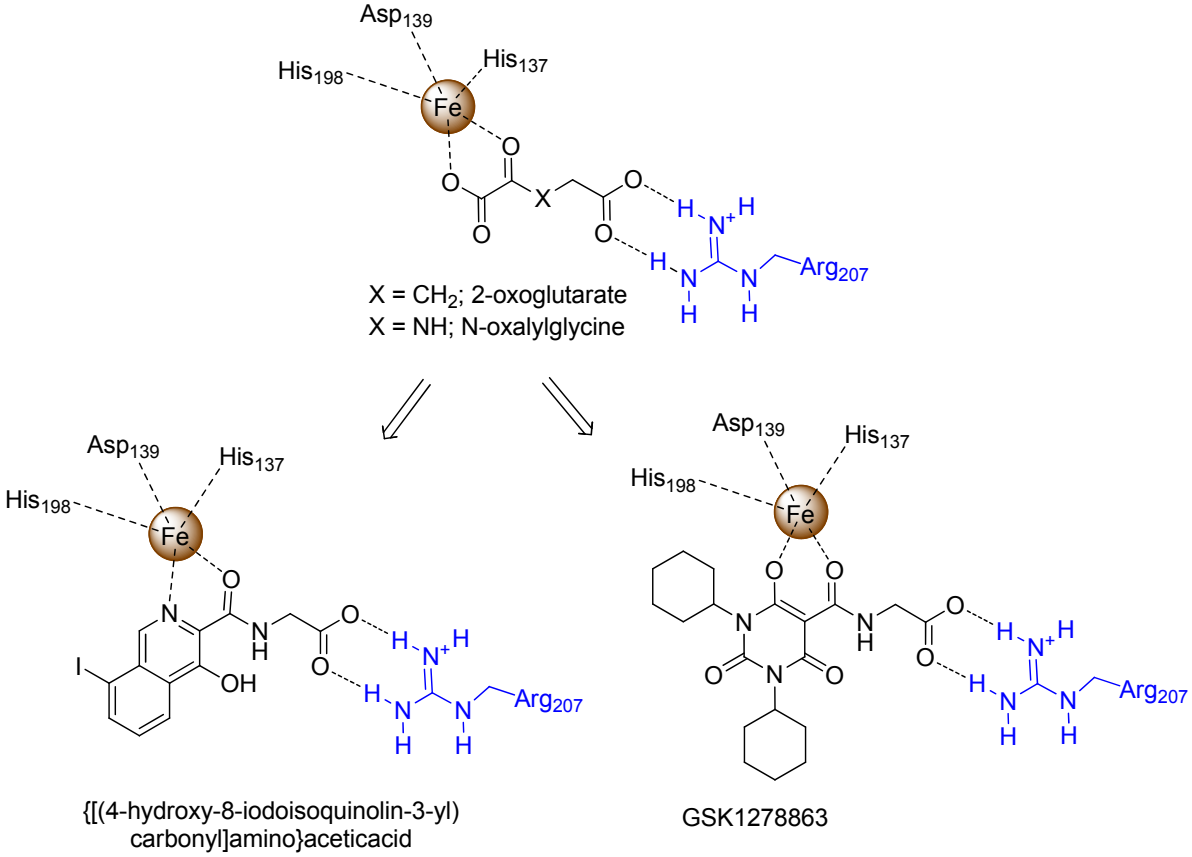

JPET Fast Forward. Published on September 19, 2017 as DOI: 10.1124/jpet.117.242503
This article has not been copyedited and formatted. The final version may differ from this version.

Figure 3

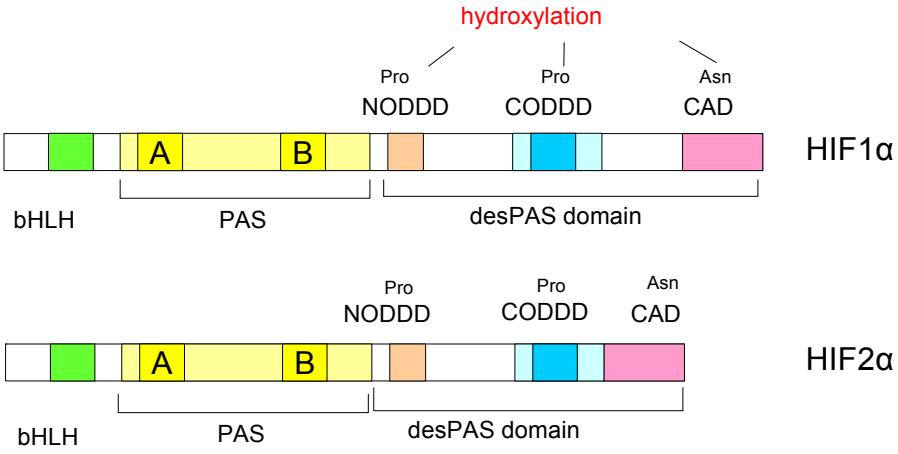

JPET Fast Forward. Published on September 19, 2017 as DOI: 10.1124/jpet.117.242503
This article has not been copyedited and formatted. The final version may differ from this version.

Figure 4

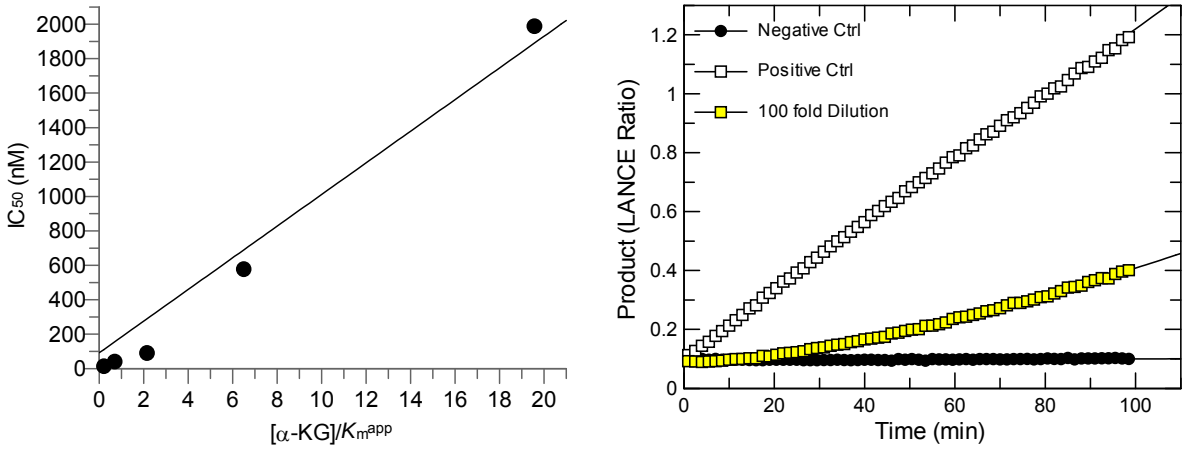

Figure 5

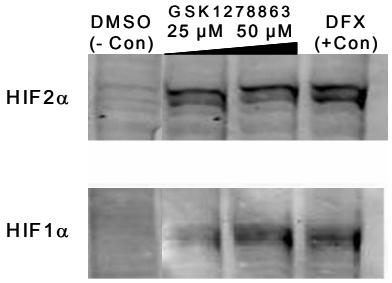

JPET Fast Forward. Published on September 19, 2017 as DOI: 10.1124/jpet.117.242503
This article has not been copyedited and formatted. The final version may differ from this version.

Figure 6

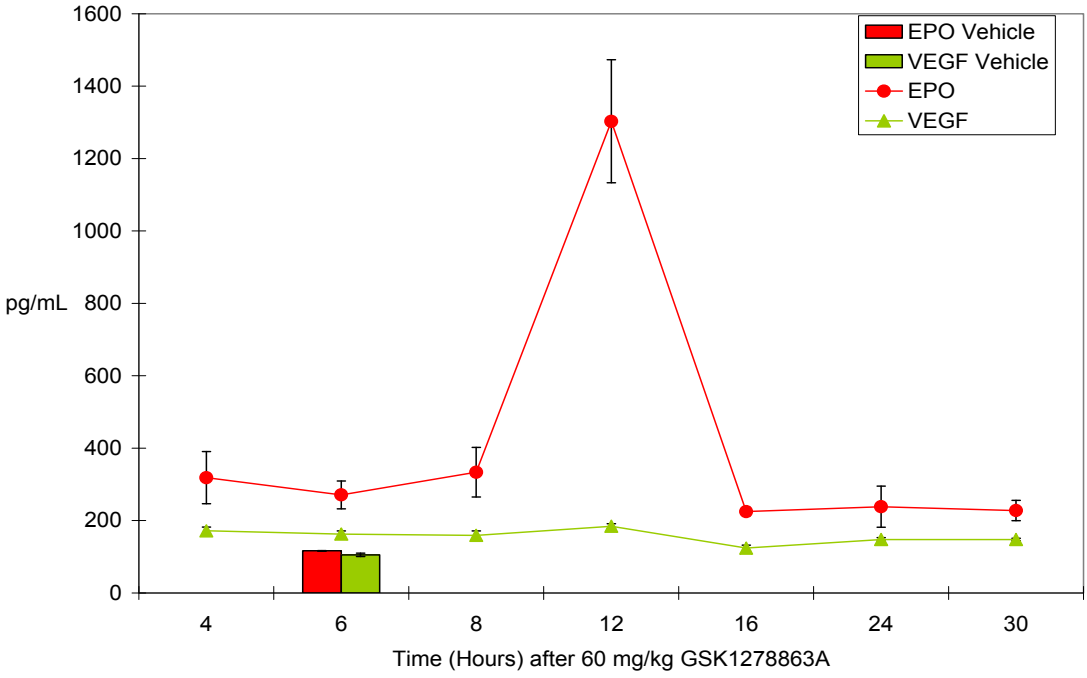

JPET Fast Forward. Published on September 19, 2017 as DOI: 10.1124/jpet.117.242503
This article has not been copyedited and formatted. The final version may differ from this version.

Figure 7

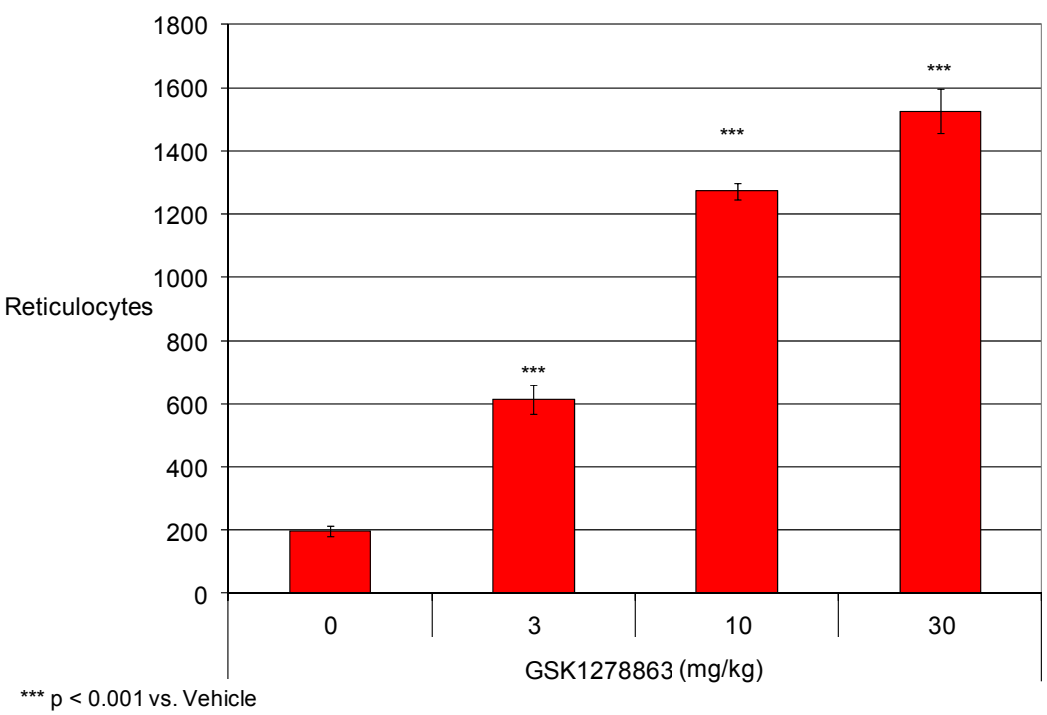

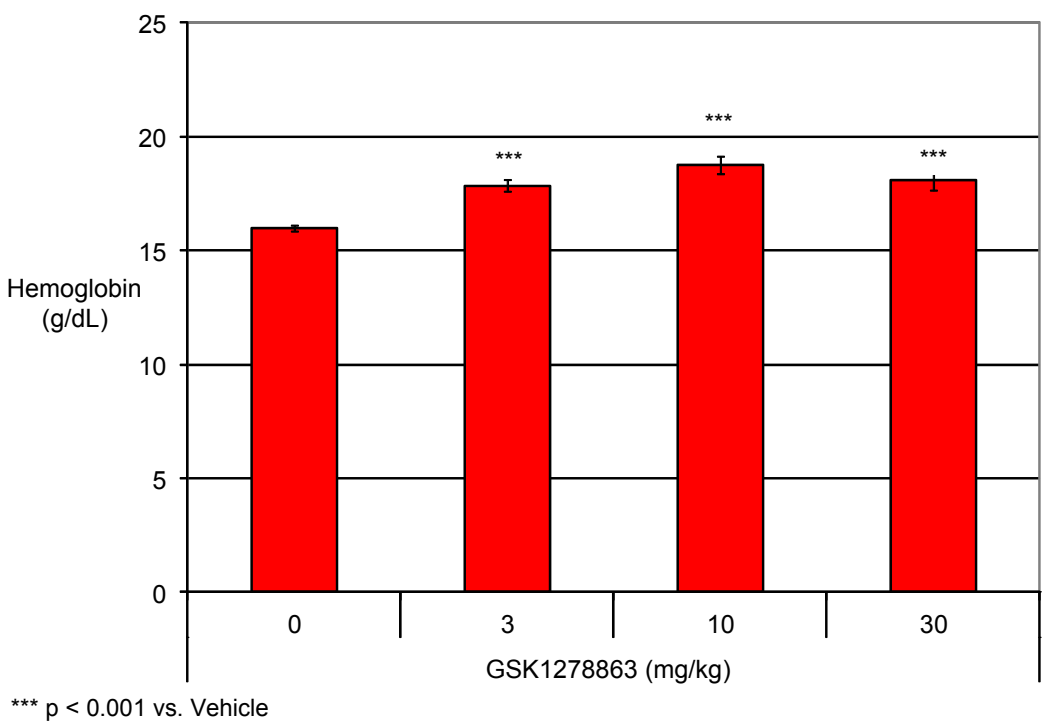

JPET Fast Forward. Published on September 19, 2017 as DOI: 10.1124/jpet.117.242503
This article has not been copyedited and formatted. The final version may differ from this version.

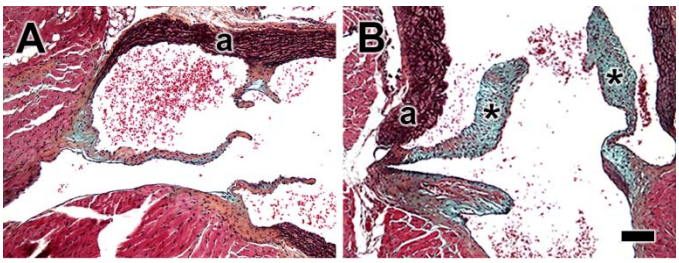

Figure 8